Full-dimensional quantum calculations of the dissociation energy, zero-point, and 10 K properties of H 7 + / D 7 + clusters using an ab initio potential energy surface

Patricia Barragán, Ricardo Pérez de Tudela, Chen Qu, Rita Prosmiti, and Joel M. Bowman

Citation: The Journal of Chemical Physics **139**, 024308 (2013); doi: 10.1063/1.4812557
View online: http://dx.doi.org/10.1063/1.4812557
View Table of Contents: http://scitation.aip.org/content/aip/journal/jcp/139/2?ver=pdfcov
Published by the AIP Publishing

Full-dimensional quantum calculations of the dissociation energy, zero-point, and 10 K properties of H_7^+/D_7^+ clusters using an *ab initio* potential energy surface

Patricia Barragán,[1] Ricardo Pérez de Tudela,[2] Chen Qu,[3] Rita Prosmiti,[1,a)] and Joel M. Bowman[3,b)]

[1]*Instituto de Física Fundamental, IFF-CSIC, Serrano 123, 28006 Madrid, Spain*
[2]*Departamento de Química Física I, Facultad de Ciencias Químicas, Universidad Complutense de Madrid, 28040 Madrid, Spain*
[3]*Department of Chemistry and Cherry L. Emerson for Scientific Computation, Emory University, 1515 Dickey Drive, Atlanta, Georgia 30322, USA*

(Received 1 May 2013; accepted 16 June 2013; published online 11 July 2013)

Diffusion Monte Carlo (DMC) and path-integral Monte Carlo computations of the vibrational ground state and 10 K equilibrium state properties of the H_7^+/D_7^+ cations are presented, using an *ab initio* full-dimensional potential energy surface. The DMC zero-point energies of dissociated fragments $H_5^+(D_5^+)+H_2(D_2)$ are also calculated and from these results and the electronic dissociation energy, dissociation energies, D_0, of 752 ± 15 and 980 ± 14 cm^{-1} are reported for H_7^+ and D_7^+, respectively. Due to the known error in the electronic dissociation energy of the potential surface, these quantities are underestimated by roughly 65 cm^{-1}. These values are rigorously determined for first time, and compared with previous theoretical estimates from electronic structure calculations using standard harmonic analysis, and available experimental measurements. Probability density distributions are also computed for the ground vibrational and 10 K state of H_7^+ and D_7^+. These are qualitatively described as a central H_3^+/D_3^+ core surrounded by "solvent" H_2/D_2 molecules that nearly freely rotate.
 [http://dx.doi.org/10.1063/1.4812557]

I. INTRODUCTION

The cationic hydrogen clusters, H_{2n+1}^+, with $n \geq 1$, and their deuterated isotopes have attracted for decades the attention of both theorists and experimentalists,[1–10] due to their presence in a series of phenomena, for example, solvation mechanisms in liquids, and nucleation dynamics models in plasma environments.

Recently, additional major motivation for research on the odd-numbered systems comes from their importance in the low-temperature interstellar chemistry reaction mechanisms.[11,12] The first member of the series, H_3^+, has been identified in the interstellar medium[13] and has been the object of much experimental and theoretical research.[14,15] The next-in-order cation, H_5^+, has been the challenging subject of laboratory observations and theoretical investigations. These investigations must of course precede a search for this cation in the interstellar medium. Apart from the earlier vibrational predissociation spectra of the H_5^+,[16,17] new infrared (IR) absorption spectra have been reported by Duncan and co-workers[18,19] from single- and multiple-photon photodissociation experiments for both H_5^+ and D_5^+ clusters, and contribute to the increased interest for theoretical studies on these cations.[20–29]

Higher order clusters of this odd-numbered series have also been experimentally observed up to H_{47}^+,[1] and more recently up to H_{119}^+ in ultracold helium nanodroplets.[30] According to experimental studies from mass spectra,[17] infrared predissociation spectroscopy,[16] and measured dissociation enthalpies,[2,3,31–33] a shell structure model has been proposed for these clusters, consisting of a H_3^+ core "solvated" by weakly bound H_2 molecules. This finding is supported by electronic structure calculations[9,34,35] and *ab initio* path integral molecular dynamics simulations.[36] Very recently, Duncan and co-workers have revisited the infrared action spectra of H_7^+, D_7^+, H_9^+, and D_9^+ above their dissociation thresholds in the 2000–4500 cm^{-1} region,[37] and made some assignments based on scaled double-harmonic Density Functional Theory (DFT) calculations of the IR spectrum.

From the theoretical point of view, the majority of studies of H_7^+ have been limited to the *ab initio* electronic structure determination of the lowest energy configuration followed by a harmonic frequency analysis. While such an approach is often adequate for semi-rigid molecules, it is generally not adequate for highly floppy molecular systems, and more sophisticated treatments are required to characterize them.

For such systems, a rigorous approach starts with an accurate, full-dimensional representation of the potential energy surface (PES). This can be either using a direct evaluation of the PES, as was done recently for H_7^+,[38] using DFT with a specific parameterization of the widely used B3LYP functional, namely B3(H),[39] based on molecular properties of such systems.[23,40] The DFT PES provides a globally correct representation of the H_7^+ cluster, suitable for direct dynamics calculations, although computationally much more demanding

a)E-mail: rita@iff.csic.es
b)E-mail: jmbowma@emory.edu

than the analytical surface. Very recently, such a PES has been reported.[41] This PES is based on higher level *ab initio* MP2 electronic energies, and fit using the invariant polynomial method of Braams and Bowman,[42] to deal with the high dimensionality and permutational symmetry of the system.

Given the availability of this accurate and computationally efficient PES for the H_7^+ cluster,[41] and motivated by the new experimental investigations on these systems,[37] we undertook diffusion Monte Carlo (DMC) and path integral Monte Carlo (PIMC) calculations to determine rigorous dissociation energies and characterizations of the zero-point and the 10 K thermal properties of H_7^+ and D_7^+. We report the results here and compare them to previous calculations and available experimental data. In Sec. II we briefly describe the newer version of the PES, which has been extended in order to more accurately describe the dissociation to the $H_5^+ + H_2$ fragments. Following that, the computational details of the DMC and PIMC calculations are presented. The results of these simulations are discussed in Sec. III, and a summary and concluding remarks are given in Sec. IV.

II. COMPUTATIONAL DETAILS

A. Potential energy surface

As mentioned above, an analytical *ab initio* PES is available for H_7^+.[41] This PES was a fit to 159 951 *ab initio* MP2/cc-pVQZ energies, employing the invariant polynomial method.[42] Briefly, a single expression containing a seven-body term was used to represent the potential function, in a permutationally invariant basis of functions of Morse-type variables for all internuclear distances, which explicitly describes the complete molecular symmetry with respect to the interchange of H atoms. This fit is a precise representation of the H_7^+ surface up to energies of about 30 000 cm^{-1}, with an overall root mean square (rms) fitting error of 170 cm^{-1}. However, during the dynamics simulations we found that at some dissociating configurations, corresponding mainly to long distances of the $H_5^+ + H_2$ or $H_3^+ + 2H_2$ fragments, the PES was not accurate, and thus we extended it to correctly describe such geometries. To do so, 12 333 new MP2 energies[43] were added to the previous database to give a total of 172 284 energies, with 8820 of them lying at energies above 20 000 cm^{-1}. The precision of the new PES was determined by the rms fitting error, stationary point analysis, and asymptotic dissociation properties. In Figure 1 the rms fitting error is presented *vs* the MP2 energies, relative to the global minimum value, and in the inset plot the number of configurations included in the fit up to the indicated energy is shown. As seen, the rms error increases as the energy increases, and we obtained an error of 110.5 cm^{-1} for energies up to 10 000 cm^{-1}, 151.4 cm^{-1} for energies below 20 000 cm^{-1}, 159.5 cm^{-1} for energies below 30 000 cm^{-1}, and an overall error of 167.5 cm^{-1}. We also indicate the zero-point energies of H_7^+ and $H_5^+ + H_2$. The average potential value is roughly half the ZPE and thus is roughly 5000 cm^{-1} and at that energy the rms fitting error is roughly 60 cm^{-1}. The effect of this fitting error on the ZPEs is difficult to determine because the PES has both positive and negative deviations from the data, and this can result in some error cancellation in the calculation of the ZPEs. Thus, while this fitting error does contribute to the uncertainty in the ZPEs and dissociation energies, D_0, we estimate that it is roughly within the statistical uncertainties given below for these energies.

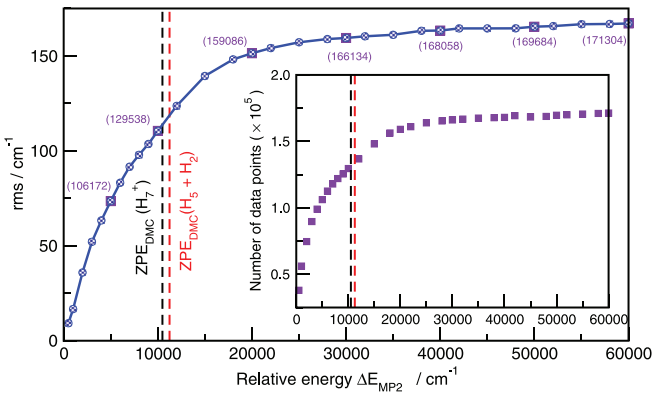

FIG. 1. Root-mean-square error and the number of configuration data (see inset plot) of the H_7^+ PES as a function of relative MP2 energy values with respect to the global minimum one. The number of configurations below the energies of 5000, 10 000, 20 000, 30 000, 40 000, 50 000, and 60 000 cm^{-1} are shown in parentheses, and the ZPE values of the H_7^+ and its fragments from the DMC calculations are plotted with dashed lines.

In Figure 2 we depict the global potential minimum structure of H_7^+, which is of C_{2v} symmetry, and has a total energy of −3.690083 a.u. on the present PES, just 1.8 cm^{-1} lower in energy than the corresponding optimized structure from the MP2/cc-pVQZ calculations.[41] The next nine stationary points in order of increasing energy are located on the current PES. Their ordering, energies, and structures are listed in comparison with their MP2 analogs in the supplementary material.[44] Normal-mode frequency analysis was also carried out for each stationary point and the results and order of the saddle point are also given in the supplementary material.[44] As in the previous fit, the energies of the two lowest saddle points, of 2-C_s and 3-C_{2v} symmetry corresponding to planar orientations of one and both H_2, respectively, differ by only about 120 cm^{-1}, while the remaining ones have energies above 800 cm^{-1}. The present PES also underestimates the electronic dissociation energy D_e by ∼65 cm^{-1}, compared to the CCSD(T)-CBS value of 1790.9 cm^{-1}.[41] We also

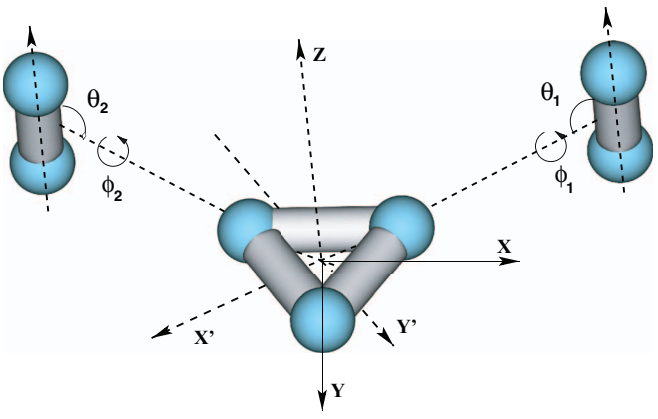

FIG. 2. Equilibrium 1-C_{2v} structure and coordinates used for the H_7^+.

examined the fragmentation behavior of the current PES, and we find a very similar overall picture as the previous PES we published.[41] Thus, we conclude that, in general, no significant differences are found between the two fits at energies up to 20 000 cm^{-1}. However, the present fit has remedied the problematic dissociative configurations and the DMC and PIMC calculations now proceed without any numerical issues. Note that this figure also gives the coordinates used for analysis of the DMC and PIMC distributions, reported below.

B. DMC and PIMC simulations

Diffusion Monte Carlo is a powerful method to determine the zero-point wavefunction and energy of a system.[45–47] It solves in a statistical way the time-dependent Schrödinger equation in imaginary time, τ. For each of the systems studied 20 000 walkers were propagated for 10 000 steps with step size, $\Delta\tau$, of 5 a.u. The average value for the energy is given by $\langle E(\tau)\rangle = \langle V(\tau)\rangle - \alpha\frac{N(\tau)-N(0)}{N(0)}$, where $\langle V(\tau)\rangle$ is the average potential energy, $\alpha = \frac{1}{\Delta\tau} = 0.2$ a.u. is found to effectively control the number of diffusing walkers, and thus the fluctuations of the $\langle E(\tau)\rangle$, and $N(\tau)$ is the number of walkers at each time τ. For H_7^+ and D_7^+ the simulations were started at the equilibrium configuration, corresponding to the global minimum of the PES, while for the $H_5^+(D_5^+)$ and $H_2(D_2)$ fragments we initiated the simulations with the fragments at their equilibrium structures and separated by 15 Å. The convergence of the DMC calculations of the ZPEs was also tested with step sizes of 2.5 and 7.5 a.u., with changes of 2 and 3 cm^{-1}, respectively, compared to those with $\Delta\tau = 5$ a.u. Such differences are within the statistical errors in the present calculations, thus the step size of 5 a.u. is used. We first allowed each of the systems to equilibrate, i.e., approach the final energy, for 2000 steps, and the energies in the remaining 8000 steps were collected for the average of a given trajectory. Five independent trajectories were calculated for each system, and the final reported value is the average over all these five trajectories. The ZPE was obtained for each of these systems and then averaged over the 5 simulations. Statistical uncertainties were obtained in usual way from these five "samples."

Path integral Monte Carlo is a quantum statistical mechanical method to evaluate thermochemical properties of molecular systems. The expectation value of the total energy is evaluated as $\langle E\rangle \equiv \frac{\int dr_1\cdots dr_M\ \varepsilon_T\ e^{-\beta V_C}}{\int dr_1\cdots dr_M\ e^{-\beta V_C}}$, where $dr_1\cdots dr_M$ are sampled according to V_C, ε_T is the thermodynamic kinetic energy estimator,[48] and V_C is the propagator potential, including both the potential values of each of M beads, and the harmonic inter-bead potential.[49] We used values of M up to 2000 for the numerical evaluation of the density operator at temperature T = 10 K. The multidimensional integrals were calculated via Metropolis Monte Carlo, and the staging sampling technique was used to perform collective movements.[50] Simulations for a total number of 2×10^7 steps were carried out for each system for M = 500, 800, 1000, 1200, 1500, and 2000. The reported PIMC energy values were obtained by extrapolating to the $M \to \infty$ limit using a quadratic fit of the type $a_0 + a_1/M^2$.[51]

III. RESULTS

A. DMC results: Zero-point and dissociation energies

DMC calculations, as described above, were performed for both H_7^+ and D_7^+ and their corresponding fragments, and accurate ZPEs were determined for all of these systems. In Table I we list the DMC values. The average value of the ZPE of H_7^+, over five different DMC simulations, is 10 490 cm^{-1} with a standard deviation of 10 cm^{-1}, while for the H_5^+ and H_2 fragments the total ZPE is 11 242 cm^{-1} with a standard deviation of 5 cm^{-1}. These results provide a dissociation energy, D_0, of 752 ± 15 cm^{-1} for the H_7^+ cluster. For the D_7^+ and

TABLE I. Anharmonic ZPEs, relative $\langle E\rangle$, D_0 dissociation energies obtained from the present DMC and PIMC calculations at T = 10 K, and their comparison with previous theoretical estimates from CCSD(T) and MP2 calculations,[35,41] and experimental values available[2,3,31,32] for the ΔH at temperatures between 25 and 330 K. Energies and enthalpies are given in cm^{-1} and temperature (in square brackets), T, in K.

	ZPE/relative $\langle E\rangle$[T]			D_0/D_0[T]			
	This work		Harmonic theory	This work		Theory	ΔH
Cluster	DMC	PIMC	CCSD(T)/MP2	DMC	PIMC	CCSD(T)-CBS	Expt.
H_7^+	10 490 ± 10/···	···/10 549 ± 19[10]	10812.5[a]/11031[b]/···	752 ± 15/··· 817[d]/···	···/766 ± 35[10] ···/831[10][d]	827/983[149.5][a]	···/1154 ± 70[c] ···/1048 ± 35[e] ···/1434[f] ···/630[g]
$H_5^+ + H_2$	11 242 ± 5/···	···/11 315 ± 16[10]	···	···	···	···	···
D_7^+	7530 ± 8/···	···/7559 ± 13[10]	···	980 ± 14/··· 1045[d]/···	···/1036 ± 21[10] ···/1101[10][d]	···	··· ···
$D_5^+ + D_2$	8510 ± 6/···	···/8595 ± 8[10]	···	···	···	···	···

[a]From Ref. 35.
[b]From Ref. 41.
[c]From Ref. 32.
[d]Corrected values by 65 cm^{-1} to account for the underestimate of the D_e in the PES compared to the CCSD(T)-CBS value.[41]
[e]From Ref. 31.
[f]From Ref. 3.
[g]From Ref. 2.

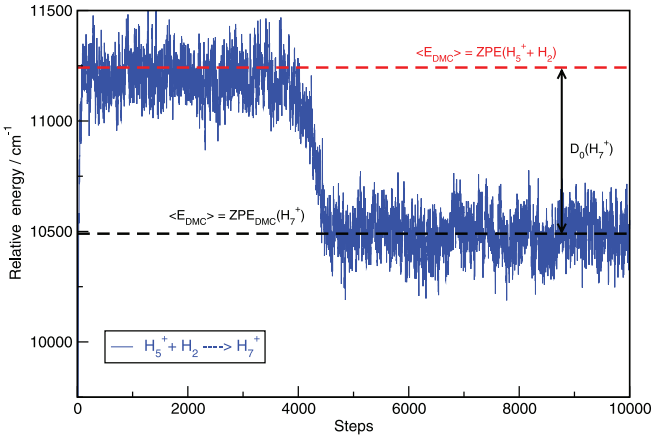

FIG. 3. DMC simulation starting from the $H_5^+ + H_2$ fragments and ends at H_7^+. The calculated ZPEs and D_0 values are also indicated.

$D_5^+ + D_2$ systems DMC simulations were also performed, and average ZPE values of 7530 ± 8 cm^{-1} and 8510 ± 6 cm^{-1}, respectively, were obtained. Thus, the corresponding D_0 value is 980 ± 14 cm^{-1}. In Figure 3 we show the imaginary time evolution of an illustrative DMC trajectory, initiated from the H_5^+ and H_2 separated fragments, and after about 4500 time steps ends in the H_7^+ complex. The dissociation energy D_0 can also be determined directly from this trajectory.

In Figure 4, the vibrational ground state wavefunction from the DMC calculations is plotted for H_7^+ and D_7^+. This was obtained as follows. We optimally aligned all the walkers from the five DMC trajectories (about 100 000 walkers) to the reference configuration shown in Figure 2, and then we divided the space into small volume elements, and counted how many times an H atom is in this volume. In this way, we obtain the amplitude of the wavefunction in that small volume. The wavefunction is represented by an isosurface. The wavefunction has the same amplitude at any point on this surface, and the isovalue of the H_7^+ is 0.028311, while for the D_7^+ is 0.039598 corresponding to 55% of the maximum value of their respective wavefunctions. From these plots, we see significant amplitude for the torsional motion of the two H_2 units, which indicates that the H_2 units are highly delocalized and behave like nearly free rotors. On the other hand, the amplitude of the H_3^+ core is relatively localized. The result is similar for the D_7^+, with, however, more localization, as expected.

B. PIMC results: Thermal equilibrium states at 10 K

Next, we report the PIMC simulations of the H_7^+, D_7^+ and their fragments at a temperature of 10 K. In Table SII (see supplementary material)[44] we list the average values of the kinetic, potential, and total energy for each system obtained using different number of beads from $M = 500$ up to 2000, and the extrapolation of the total energy to the $M \to \infty$ limit. The relative $\langle E \rangle$ values at 10 K as a function of the number of beads and their extrapolations, using the quadratic expression mentioned above, are plotted in Figures 5 and 6 for the $H_7^+/H_5^+ + H_2$ and $D_7^+/D_5^+ + D_2$, respectively. The extrapolated energy values, listed in Table I, are 10 549 ± 19 cm^{-1} and 11 315 ± 16 cm^{-1} for the H_7^+ and $H_5^+ + H_2$, and their difference gives a dissociation energy value at T = 10 K of 766 ± 35 cm^{-1}. For the D_7^+ and $D_5^+ + D_2$ the relative $\langle E \rangle$ values at 10 K are 7559 ± 13 and 8595 ± 8 cm^{-1}, respectively, and thus a dissociation energy at T = 10 K of 1036 ± 21 cm^{-1} (see Table I) is obtained.

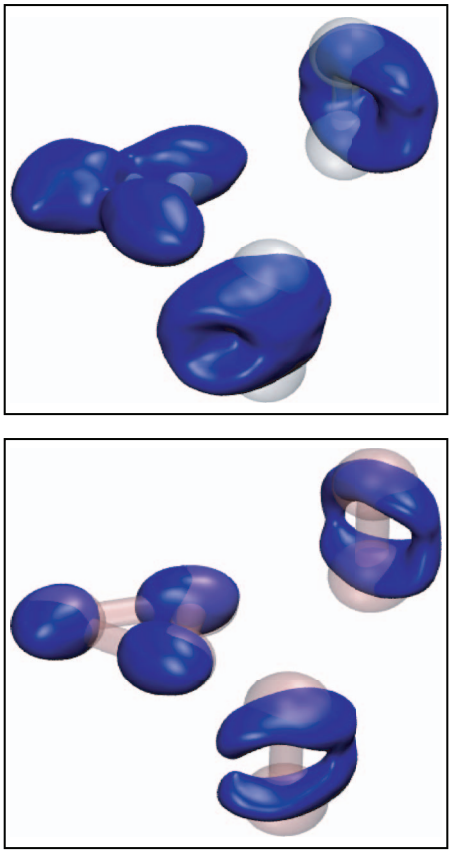

FIG. 4. Isosurfaces of the vibrational ground state wavefunction for the H_7^+ (top panel) and D_7^+ (bottom panel) from the DMC calculations (see the text for details).

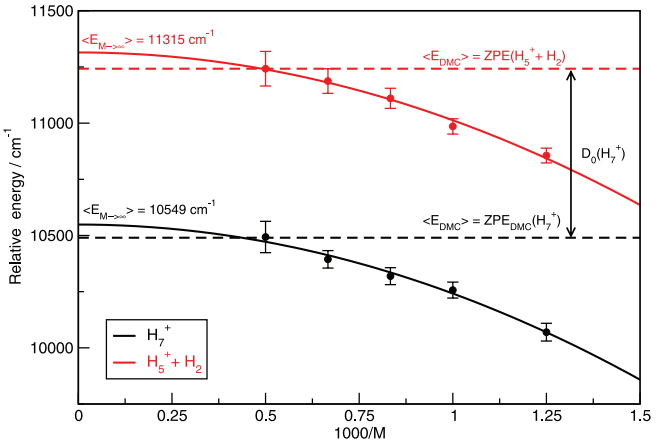

FIG. 5. Averaged relative (to the global minimum) energies (in cm^{-1}) as a function of the number of beads and their error (filled circles), and extrapolation (solid lines) to the $M \to \infty$ limit for the H_7^+ and $H_5^+ + H_2$ fragments from the PIMC calculations at T = 10 K. The calculated ZPEs and D_0 values from the DMC simulations (dashed lines) are also shown.

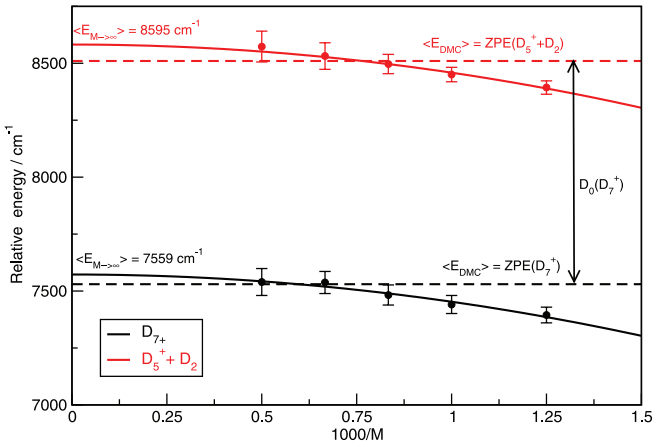

FIG. 6. Same as Fig. 5, but for the D_7^+ and $D_5^+ + D_2$.

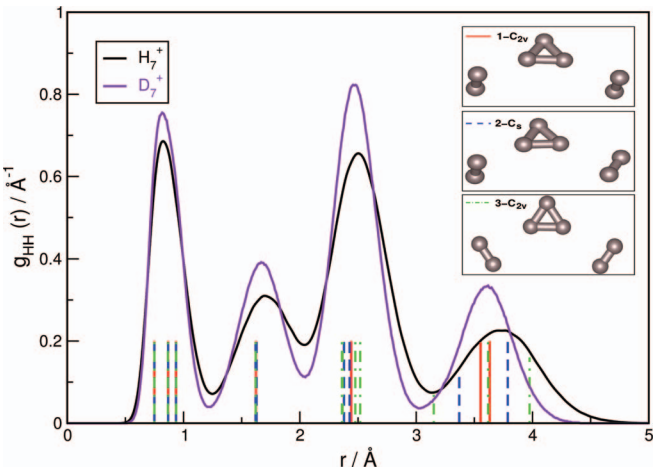

FIG. 7. Radial HH pair distribution functions of the thermal equilibrium states of the H_7^+ (black line) and D_7^+ (purple color line) at T = 10 K. The vertical lines correspond to the HH bondlengths of the indicated 1-C_{2v}, 2-C_s, and 3-C_{2v} structures.

From the PIMC calculations with $M = 2000$, we computed radial and angular distribution functions for the thermal equilibrium state of the H_7^+ and D_7^+ clusters. In Figure 7, we present the radial HH/DD pair distribution functions for H_7^+/D_7^+. Also we display in Fig. 7 the different HH distances (see vertical bar lines) of the 1-C_{2v} global minimum configuration, and the lowest two 2-C_s and 3-C_{2v} saddle points. As we mentioned above in Sec. II A, these stationary points correspond to a 90° rotation of the H_2 molecules (see ϕ_1 and ϕ_2 angles in Fig. 2). The 2-C_s structure lies at 45.2 cm^{-1} above the global minimum, and corresponds to a rotation of only one H_2 molecule, while the 3-C_{2v}, one at energy of 122.8 cm^{-1}, corresponds to a planar configuration with both H_2 molecules in the same plane as the H_3^+ core (see the inset plot in Fig. 7). Both HH/DD pair distribution functions show four peaks that correspond to the HH bondlengths of the three stationary points of the PES. The first peak in the 0.7–1.0 Å range is associated with the interatomic distances in the H_2 and H_3^+ units; the second and third peaks at 1.7 and 2.5 Å, respectively, for the distances between the atoms in the H_3^+ and H_2, while the last peak centered at 3.7 Å for the distances between the atoms in the two H_2 moieties. The first peak is the narrowest one, indicating that the H_3^+ and H_2 units are more localized than their relative orientations and distances. Also, as expected, the pair distribution for H_7^+ is much broader than the D_7^+ one, and for longer HH distances the peaks are shifted to larger values, mainly due to the overall extension of the H_7^+ compared to the D_7^+.

For a more quantitative analysis in characterizing the thermal equilibrium state H_7^+ and D_7^+, we also computed angular distribution functions. In Figure 8 we present the ones in the $\theta_{1,2}$ and in $\phi_{1,2}$, where $\theta_{1,2}$ are the angles formed by each of the vectors along the H_2 and the one connecting their center of masses with the closest H atom of the H_3^+, while $\phi_{1,2}$ are the torsional angles corresponding to the rotations of the H_2 (see Fig. 2). One can see that the $D(\theta)$ distributions show a broad peak at 90° extending from 60° to 120°, indicating the delocalization of the librations of the two H_2 or D_2 about the C_2 axes, while the $D(\phi)$ distribution functions are much more extended over the whole range, indicating quantum large amplitude H_2/D_2 torsions. In Figure 9, 2D contour plots of the probability density distribution of the thermal equilibrium state of the H_7^+ in Cartesian coordinates are displayed. By projecting the distribution onto the H_3^+-plane (see Fig. 2) one can clearly see the higher localization of the H_3^+

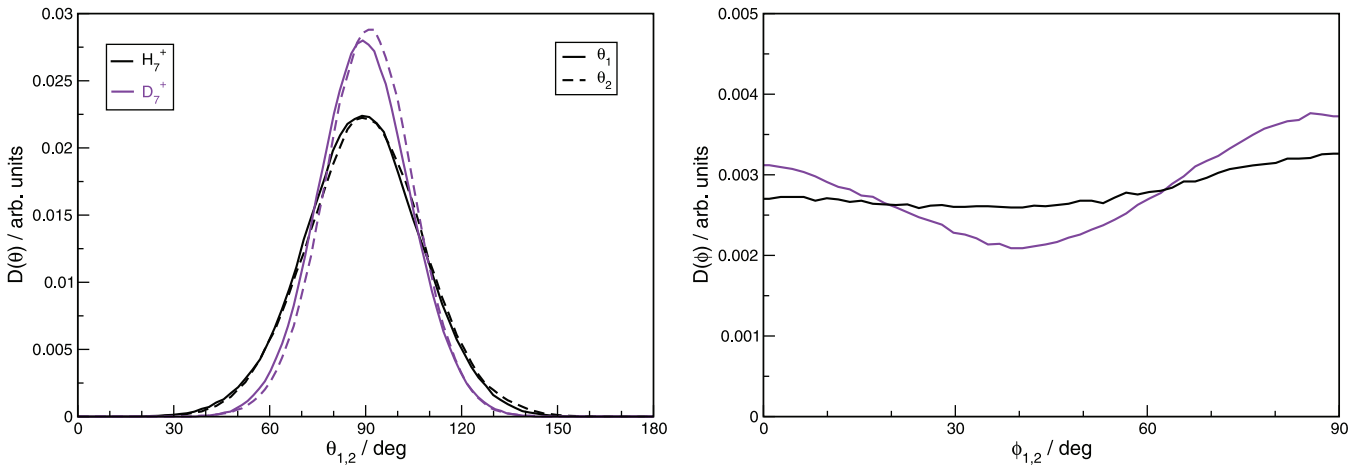

FIG. 8. Angular, in θ (left panel) and ϕ (right panel), distribution functions of the thermal equilibrium states of the H_7^+ and D_7^+ at T = 10 K.

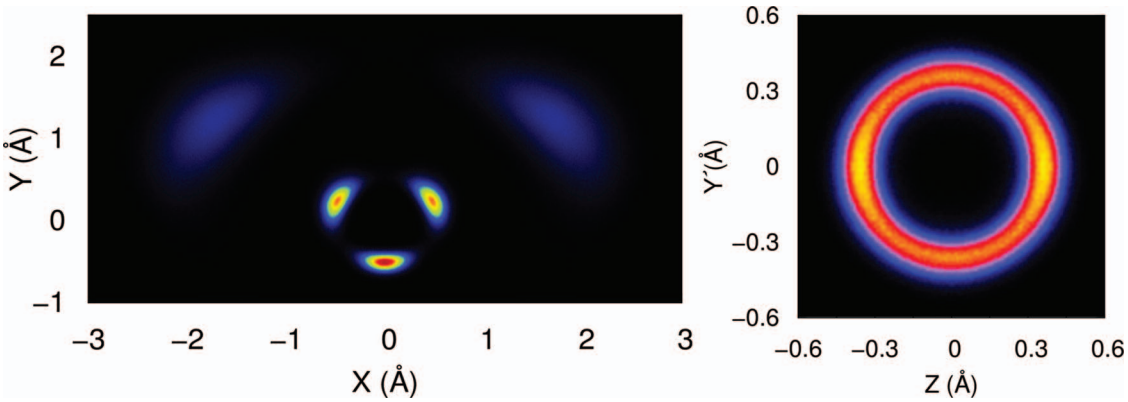

FIG. 9. Contour plots of the probability density distributions at T = 10 K of the H_7^+ projected onto the H_3^+ plane (left panel), and of both H_2 moieties projected onto their rotation planes (right panel) are shown.

core compared to the librations of the H_2, while by projecting the distribution onto the rotation plane of the H_2 we show the delocalization of their torsional motion. Further, for a more quantitative analysis, the rigidity of the H_7^+ and D_7^+ structures is also characterized by examining the root-mean-square bondlength and angular fluctuations, in terms of the system-averaged Lindemann index,[52] $\delta = \frac{1}{N(N-1)} \sum_{i \neq j} \frac{\sqrt{(\langle q_{ij}^2 \rangle - \langle q_{ij} \rangle^2)}}{\langle q_{ij} \rangle}$, where q_{ij} is the distance or angle of interest. By comparing the values obtained for the bondlength fluctuations in the H_3^+ and H_2 units we found similar values of 0.13 and 0.11, respectively, while for the angular (libration and torsion) fluctuations δ values of 0.17, 0.45 and 0.14, 0.27 are computed for the H_7^+ and D_7^+, respectively. One can see that the angular fluctuations are 2-3 times larger in H_2 units compared to the H_3^+ core.

C. Discussion

In Table I, the ZPE and $\langle E \rangle_T$ values from the DMC and PIMC calculations and the computed dissociation energies at T = 0 and 10 K are listed in comparison with previously reported theoretical and experimental data. We should point out here that from DMC calculations we obtain the D_0 values for the systems, while from the PIMC simulations we compute their dissociation energies at T = 10 K, as the difference of the $\langle E \rangle$ values of the H_7^+/D_7^+ and $H_5^+ + H_2/D_5^+ + D_2$ systems. The results of the DMC and the PIMC values are consistent with each other, with the DMC values, as it was expected, to be lower than the $M \rightarrow \infty$ values from the PIMC calculations (see Figs. 5 and 6). As we mentioned before, the ZPE and D_0 values are the first theoretical estimates in the literature from anharmonic quantum mechanical treatments for the H_7^+/D_7^+ cations. Thus, we can only compare them with the best predictions of the harmonic MP2 and CCSD(T) calculations available in the literature.[35,41] Anharmonic vibrational frequencies have been reported from MP2-VSCF calculations using 6-311G(p) basis set for the H_7^+,[53] and a direct evaluation of the potential on 2-mode grids in the normal modes. However, a ZPE value was not reported there.[53] A ZPE value of 10 812.5 cm^{-1} has been reported from CCSD(T)/aug-cc-pVQZ calculations,[35] and 11 031 cm^{-1} at the MP2/cc-pVQZ level.[41] One can see that depending on the level of theory, anharmonicity of more than 300 cm^{-1} is estimated for H_7^+. By comparing the D_0 values from the DMC and PIMC calculations with the ones from the CCSD(T)-CBS calculations,[35] using a more accurate D_e but harmonic ZPEs, we see a difference of 10%. Some of this difference comes, as we mentioned above, from the different level of theory in the *ab initio* calculations, estimated about 65 cm^{-1} in the D_e value for H_7^+.[41] Note that in the CCSD(T)-CSB calculations the D_e value has been computed by extrapolating the CCSD(T) value to its complete basis set (CBS) limit. The zero-point vibrational energies and thermal corrections have been obtained from harmonic vibrational frequency and thermodynamics analysis at CCSD(T)/aug-cc-pVQZ level for both reactants and products,[35] assuming an average temperature of 149.5 K from the experimental van't Hoff plots[32] for the H_7^+. We should also mention here that the harmonic ZPE value for the present PES is 11 061 cm^{-1} that compares very well with the previously reported value of 11 031 cm^{-1} from the MP2 computations.[41] One can see that the ZPE predicted by the PES is higher than the corresponding *ab initio* value by 30 cm^{-1}, within the rms error of the PES's parameterization.

In Table I, we also present the experimental $-\Delta H$ values reported for the clustering $H_5^+ + H_2 \rightarrow H_7^+$ reaction,[2,3,31,32] over a temperature range of 25–330 K. The most recent studies,[31,32] over 20 years old, report values of 1154 ± 70 and 1048 ± 35 cm^{-1}, respectively, and these are quite different from the earlier reported ones of 1434 and 630 cm^{-1}.[2,3] So, clearly, there is significant experimental uncertainty here. The present results are for D_0 = 752 ± 15 cm^{-1}, from DMC calculations, and 766 ± 35 cm^{-1} at 10 K, from PIMC calculations. As indicated in Table I, we give the directly calculated values of the quantities as well as the corrected ones by adding 65 cm^{-1} to these to account for the MP2 difference in D_e compared to the most accurate CCSD(T)-CBS result. Note that the present calculated quantities are not directly comparable to experiment, which give the negative of the enthalpy of formation at temperatures between 25 and 330 K. We do not calculate the enthalpy ΔH, however, at 10 K the difference between ΔH and $\Delta \langle E \rangle$ is quite small and we estimate (using the ideal gas approximation) that it is within the statistical uncertainties of the PIMC and DMC calculations. The difference between the PIMC value in particular and ΔH of roughly 200 cm^{-1} could almost be accounted for by the

uncertainties in both theory and experiment. In any case, we are confident that the present calculations of dissociation energy at T = 0 and 10 K are the most accurate ones reported to date.

Considxering now the structural properties of the quantum vibrational ground and 10 K equilibrium states of the H_7^+ and D_7^+ from the DMC and PIMC simulations, respectively, we found that they correspond to a much more localized H_3^+ core than the two H_2 units, which undergo large-amplitude torsions with probability at planar structures such as the 2-C_s and 3-C_{2v} ones (see Figs. 4, 7, and 9). This finding is in qualitative agreement with the quantum structural fluctuations predicted by previous path integral molecular dynamics simulations combined with DFT electronic structure calculations at low temperature.[36] Such quantum torsional delocalization has also been found for the H_5^+ and D_5^+ ground states.[18,21,24,26] However here, based on the DMC (see Fig. 4) and PIMC (see the left panel of Fig. 9) results for the H_7^+ and D_7^+, we did not observe any significant exchange of the proton between the H_3^+ and H_2 subunits. In addition to these visualizations, in the DMC simulations we keep track of the internuclear distances of the walkers to monitor exchange, and we do not see any, confirming an H_3^+-solvated structure.

We note that the shared-proton exchange motion (the exchange of the central proton between the two H_2 groups) plays an important role in the assignment of the extremely rich IR spectra of the H_5^+ and H_5^+ cations.[18,19,25–28] Thus, the lack of such exchange in the H_7^+ case might give rise to simpler vibrational patterns. However, even here, the standard scaled double-harmonic analysis, used by Duncan and co-workers[37] to model their recent H_7^+ and D_7^+ IR spectra, does indicate some possible underlying issues, especially for the highest frequency fundamental, where experiment is significantly below the calculation. While the present calculations for the ground vibrational and the 10 K thermal states do not address these experiments, they do provide important insight into the nature of the initial state for any rigorous calculation of the IR spectrum, and thus they do provide some guidance on how to address a rigorous calculation of this spectrum, especially for the low-frequency modes.

IV. SUMMARY AND CONCLUSIONS

We reported a theoretical investigation of the vibrational ground and 10 K equilibrium states of the H_7^+ and D_7^+ clusters using diffusion Monte Carlo and path integral Monte Carlo simulations on a new *ab initio* full-dimensional PES, fitted to MP2 energies employing the invariant polynomial method. Both approaches are in agreement with each other, showing that the proton is localized in the H_3^+ core, while the H_2 units are highly delocalized in their torsional motions that span the three lowest stationary points of the PES: 1-C_{2v}, 2-C_s, and 3-C_{2v}. Such torsional delocalization is similar with the reported results for the H_5^+ cation. However, we did not find evidence of significant proton exchange between the outer H_2 and inner H_3^+ subunits for the H_7^+ cluster, as was found in H_5^+. In this way, for the first time anharmonic ZPEs for these cations and their fragments are determined, and as it was expected the ZPE decreases with isotopic substitution.

The dissociation energies at 0 and 10 K were also reported for H_7^+ and D_7^+. We estimated the systematic uncertainties and errors in these quantities due to the known error in the electronic dissociation energy of the PES of roughly 65 cm^{-1}, as well as statistical errors. From the DMC simulations D_0 energies of 752 ± 15 and 980 ± 14 cm^{-1} are computed, for the H_7^+ and D_7^+, respectively. Similar energy values, within the statistical errors, are also obtained from the PIMC calculations at a temperature of T = 10 K. Comparisons with available experimental data available for the $H_7^+ \rightarrow H_5^+ + H_2$ dissociation enthalpies at temperatures of 25–330 K were also made. The calculated dissociation energies at T = 10 K values show deviations from the experimental enthalpy measurements, roughly 200 cm^{-1} with the most recent one.

In the present work, we also demonstrated the importance of the nuclear quantum effect on the structural properties of these cations. Both approaches are in agreement with each other, showing that the proton is localized in the H_3^+ core, while the H_2 units are more delocalized rotationally. The nature of the ground vibrational states has been characterized, and this is an important piece of information in planning any future calculations for the excited vibrational states of these systems. Specifically, it will be of interest to investigate to what extent the H_7^+ large-amplitude torsional motions are manifest in the IR spectrum. Such studies, done rigorously, are a great challenge, as it will also be the study of quantum fluctuations in the larger H_9^+ cation, corresponding to a completed inner shell structure.

ACKNOWLEDGMENTS

The authors thank the Centro de Calculo (IFF-CSIC), and SGAI (CSIC) for allocation of computer time. C.Q. thanks NASA for financial support through Grant No. 370 NNX12AF42G from the NASA Astrophysics Research and Analysis program. This work has been supported by MICINN, Spain, Grant No. FIS2011-29596-C02-01, Consolider-Ingenio 2010 Programme CSD2009-00038 (MICINN), and COST Action CM1002 (CODECS).

[1] R. Clampitt and L. Towland, Nature **223**, 815 (1969).
[2] S. L. Bennett and F. H. Field, J. Am. Chem. Soc. **94**, 8669 (1972).
[3] K. Hiraoka and P. Kebarle, J. Chem. Phys. **62**, 2267 (1975).
[4] M. Okumura, L. I. Yeh, and Y. T. Lee, J. Chem. Phys. **83**, 3705 (1985).
[5] N. J. Kirchner and M. T. Bowers, J. Chem. Phys. **91**, 2573 (1987).
[6] R. Ahlrichs, Theor. Chem. Acta. **39**, 149 (1975).
[7] Y. Yamaguchi, J. F. Gaw, and H. F. Shaefer III, J. Chem. Phys. **78**, 4074 (1983).
[8] M. Farizon, H. Chermette, and B. J. Farizon-Mazuy, J. Chem. Phys. **96**, 1325 (1992).
[9] M. Barbatti, G. Jalbert, and M. A. C. Nascimento, J. Chem. Phys. **113**, 4230 (2000).
[10] R. Prosmiti, A. A. Buchachenko, P. Villarreal, and G. Delgado-Barrio, Theor. Chem. Acc. **106**, 426 (2001).
[11] D. Gerlich, E. Herbst, and E. Roueff, Planet. Space Sci. **50**, 1275 (2002).
[12] K. N. Crabtree, N. Indriolo, H. Kreckel, B. A. Tom, and B. McCall, Astrophys. J. **729**, 15 (2011).
[13] T. R. Geballe and T. Oka, Nature **384**, 334 (1996).
[14] T. Oka, Philos. Trans. R. Soc. London, Ser. A **370**, 4991 (2012).
[15] L. Adamowicz and M. Pavanello, Philos. Trans. R. Soc. London, Ser. A **370**, 5001 (2012); O. L. Polyansky, A. Alijah, N. F. Zobov, I. I. Mizus, R. I. Ovsyannikov, J. Tennyson, L. Lodi, T. Szidarovsky, and A. G. Császaár, *ibid.* **370**, 5014 (2012).

[16]M. Okumura, L. I. Yeh, and Y. T. Lee, J. Chem. Phys. **88**, 79 (1988).
[17]Y. K. Bae, P. C. Cosby, and D. C. Lorents, Chem. Phys. Lett. **159**, 214 (1989).
[18]T. C. Cheng, B. Bandyopadyay, Y. Wang, S. Carter, B. J. Braams, J. M. Bowman, and M. A. Duncan, J. Phys. Chem. Lett. **1**, 758 (2010).
[19]T. C. Cheng, L. Jiang, K. R. Asmis, Y. Wang, J. M. Bowman, A. M. Ricks, and M. A. Duncan, J. Phys. Chem. Lett. **3**, 3160 (2012).
[20]Z. Xie, B. J. Braams, and J. M. Bowman, J. Chem. Phys. **122**, 224307 (2005).
[21]P. H. Acioli, Z. Xie, B. J. Braams, and J. M. Bowman, J. Chem. Phys. **128**, 104318 (2008).
[22]A. Aguado, P. Barragán, R. Prosmiti, G. Delgado-Barrio, P. Villarreal, and O. Roncero, J. Chem. Phys. **133**, 024306 (2010).
[23]P. Barragán, R. Prosmiti, O. Roncero, A. Aguado, P. Villarreal, and G. Delgado-Barrio, J. Chem. Phys. **133**, 054303 (2010).
[24]R. Pérez de Tudela, P. Barragán, R. Prosmiti, P. Villarreal, and G. Delgado-Barrio, J. Phys. Chem. A **115**, 2483 (2011); P. Barragán, R. Pérez de Tudela, R. Prosmiti, P. Villarreal, and G. Delgado-Barrio, Phys. Scr. **84**, 028109 (2011).
[25]C. Sanz-Sanz, O. Roncero, A. Valdés, R. Prosmiti, G. Delgado-Barrio, P. Villarreal, P. Barragán, and A. Aguado, Phys. Rev. A **84**, 060502(R) (2011); A. Valdés, P. Barragán, C. Sanz-Sanz, R. Prosmiti, P. Villarreal, and G. Delgado-Barrio, Theor. Chem. Acc. **131**, 1210 (2012).
[26]A. Valdés, R. Prosmiti, and G. Delgado-Barrio, J. Chem. Phys. **136**, 104302 (2012); **137**, 214308 (2012).
[27]Z. Lin and A. B. McCoy, J. Phys. Chem. Lett. **3**, 3690 (2012).
[28]A. Valdés and R. Prosmiti, "Theoretical Investigation of the Infrared Spectra of the H_5^+ and D_5^+ Cations," J. Phys. Chem. A (to be published).
[29]H. Song, S.-Y. Lee, M. Yang, and Y. Lu, J. Chem. Phys. **138**, 124309 (2013).
[30]S. Jaksch, A. Mauracher, A. Bacher, S. Denifl, F. Ferreira Da Silva, H. Schöbel, O. Echt, T. D. Märk, M. Probst, D. K. Bohme, and P. Scheier, J. Chem. Phys. **129**, 224306 (2008).
[31]R. J. Beuhler, S. Ehrenson, and L. Friedman, J. Chem. Phys. **79**, 5982 (1983).
[32]K. Hiraoka, J. Chem. Phys. **87**, 4048 (1987).
[33]K. Hiraoka and T. Mori, J. Chem. Phys. **91**, 4821 (1989).
[34]H. Chermette and I. V. Ymmud, Phys. Rev. B **63**, 165427 (2001).
[35]R. Prosmiti, P. Villarreal, and G. Delgado-Barrio, J. Phys. Chem. A **107**, 4768 (2003).
[36]I. Štich, D. Marx, M. Parrinello, and K. Terakura, J. Chem. Phys. **107**, 9482 (1997).
[37]J. W. Young, T. C. Cheng, B. Bandyopadhyay, and M. A. Duncan, "IR Photodissociation Spectroscopy of H_7^+, H_9^+, and Their Deuterated Analogues," J. Phys. Chem. A (to be published).
[38]P. Barragán and R. Prosmiti, Int. J. Quantum Chem. **113**, 651 (2013).
[39]H. Chermette, H. Razafinjanahary, and L. Carrion, J. Chem. Phys. **107**, 10643 (1997).
[40]P. Barragán, R. Prosmiti, P. Villarreal, and G. Delgado-Barrio, Int. J. Quantum Chem. **111**, 368 (2011).
[41]P. Barragán, R. Prosmiti, Y. Wang, and J. M. Bowman, J. Chem. Phys. **136**, 224302 (2012).
[42]B. J. Braams and J. M. Bowman, Int. Rev. Phys. Chem. **28**, 577 (2009).
[43]H.-J. Werner, P. J. Knowles, R. Lindh, F. R. Manby, M. Schütz *et al.*, MOLPRO, version 2009.1, a package of *ab initio* programs, 2009, see http://www.molpro.net.
[44]See supplementary material at http://dx.doi.org/10.1063/1.4812557 for the energetics and the order of the ten stationary points of the PES, and average potential, kinetic, and total energy values from the PIMC calculations for the H_7^+, D_7^+, $H_5^+ + H_2$, and $D_5^+ + D_2$, as a function of the number of beads used and the extrapolation to their $M \rightarrow \infty$ limit.
[45]J. B. Anderson, J. Chem. Phys. **63**, 1499 (1975).
[46]I. Kosztin, B. Faber, and K. Schulten, Am. J. Phys. **64**, 633 (1996).
[47]A. B. McCoy, Int. Rev. Phys. Chem. **25**, 77 (2006).
[48]J. A. Baker, J. Chem. Phys. **70**, 2914 (1979).
[49]K. R. Glaesemann and L. E. Fried, J. Chem. Phys. **118**, 1596 (2003).
[50]M. Sprik, M. L. Klein, and D. Chandler, Phys. Rev. B **31**, 4234 (1985).
[51]R. E. Zillich and K. B. Whaley, J. Phys. Chem. A **111**, 7489 (2007).
[52]T. L. Beck, J. D. Doll, and D. L. Freeman, J. Chem. Phys. **90**, 5651 (1989).
[53]M. Barbatti and M. A. C. Nascimento, J. Chem. Phys. **119**, 5444 (2003).